CERN – EUROPEAN ORGANIZATION FOR NUCLEAR RESEARCH

CLIC – Note – 1142

TOLERANCE STUDY FOR ACCELERATING STRUCTURE IN THE CLIC MAIN LINAC

Jiayang Liu[1,2], Alexej Grudiev[2]

[1]Tsinghua University, Beijing, China
[2]CERN, Geneva, Switzerland

CERN-ACC-2019-0049
19/02/2019

Abstract

The tolerances are essential for defining the fabrication shape accuracy specification as well as the structure temperature control. In this paper, the tolerance study for a single accelerating structure of the CLIC main linac is described. The change in the nominal accelerating voltage caused by systematic temperature errors, systematic geometrical errors and random geometrical errors has been investigated. The tolerances related to the change in the field distribution and the reflections in the structure have also been analyzed.

Geneva, Switzerland
19 February 2019

Tolerance study for accelerating structure in the CLIC main linac

Jiayang Liu (1,2), Alexej Grudiev (2)

(1) Tsinghua University, Beijing, China

(2) CERN, Geneva, Switzerland

Abstract

The tolerances are essential for defining the fabrication shape accuracy specification as well as the structure temperature control. In this paper, the tolerance study for a single accelerating structure of the CLIC main linac is described. The change in the nominal accelerating voltage caused by systematic temperature errors, systematic geometrical errors and random geometrical errors has been investigated. The tolerances related to the change in the field distribution and the reflections in the structure have also been analysed.

I. Introduction

The Compact Linear Collider (CLIC) is a high-luminosity linear electron–positron collider covering a center-of-mass energy range from 380 GeV to 3 TeV under development [1,2]. For 3 TeV stage, the novel two-beam acceleration scheme is utilized to reduce the number of klystrons to a manageable value and to build at reasonable cost. The accelerating structure (AS) optimized for 3 TeV CLIC is named CLIC-G* [3,4] and the one designed for 380 GeV CLIC is named CLIC-380 [5]. For the first CLIC stage of 380 GeV, an alternative klystron-based scenario using X-band klystrons to produce the RF power is proposed. The accelerating structure designed for the main linac of the klystron-based CLIC is named CLIC-K [6]. The parameters of these three different structures are presented in Table. 1 for comparison.

Table 1. Parameters of CLIC-G*, CLIC-380 and CLIC-K

Parameters	CLIC-G*	CLIC-380	CLIC-K
Frequency	11.994 GHz	11.994 GHz	11.994 GHz
Average loaded Accelerating gradient	100 MV/m	72 MV/m	75 MV/m
Input RF power	62.3 MW	60.6 MW	40.6 MW
Active length	0.23 m	0.275 m	0.23 m
RF phase advance per cell	120 °	120 °	120 °
Number of cells	28	33	28
Average iris radius / RF wavelength	0.11	0.13325	0.1175
First iris radius / RF wavelength	0.126	0.1625	0.145
Last iris radius / RF wavelength	0.094	0.104	0.09
First iris thickness / cell length	0.2	0.303	0.25
Last iris thickness / cell length	0.12	0.172	0.134
Number of particles per bunch	3.72×10^9	5.2×10^9	3.87×10^9
Number of bunches per train	312	352	485

In this paper, two effects of the errors on the performance of one travelling wave accelerating structure have been investigated. The change in the nominal accelerating voltage caused by three different effects including systematic geometrical and temperature errors and random geometrical errors has been analyzed in Sec. II. The tolerances on the geometrical errors given by the acceptable reflection along the structure resulting in the change of filed distribution are described in Sec. III. In the main body of the paper, we only present the results for the CLIC-K structure. The tolerance results in CLIC-G* and CLIC-380 are summarized in Appendix I and II, respectively.

II. Tolerances given by the effect of the reduction of the nominal accelerating voltage

Accelerating voltage is one of the key performances of the accelerating structure. The errors on the

voltage will cause the deviation of the beam energy gain from the designed one. The acceptable AS-to-AS voltage error should be below ± 1% [7].

Figure 1. Schematic diagram of an accelerating structure with N cells.

For an accelerating structure with N cells shown in Figure 1, the accelerating voltage can be calculated by adding up the voltages of each cell. The accelerating voltage of cell *i* is determined by the accelerating gradient G_i and the RF phase, as expressed in Equation (1), where L_c is the cell length, φ_0 is the input RF phase and $\delta\varphi_c^i$ is the phase error of cell i. The nominal accelerating voltage is calculated by Equation (2), where φ_s is the designed RF synchronous phase. If there is no phase error in every cell, the RF input phase φ_0 should be the same as the designed RF synchronous phase φ_s. Considering the phase errors, the RF input phase φ_0 can be optimized to minimize the accelerating voltage error so that the tolerances can be less critical for the same limited voltage error, as illustrated in Figure 2. The change in the nominal accelerating voltage caused by three different effects will be analyzed in the following parts.

$$V=\sum_{i=1}^{N}V_i\,,\quad V_i=G_iL_c\cos\left(\varphi_0+\delta\varphi_i\right),\quad \delta\varphi_i=\sum_{j=1}^{i}\delta\varphi_c^j \tag{1}$$

$$V_a=V_0\cos\left(\varphi_s\right),\quad V_0=\sum_{i=1}^{N}G_iL_c \tag{2}$$

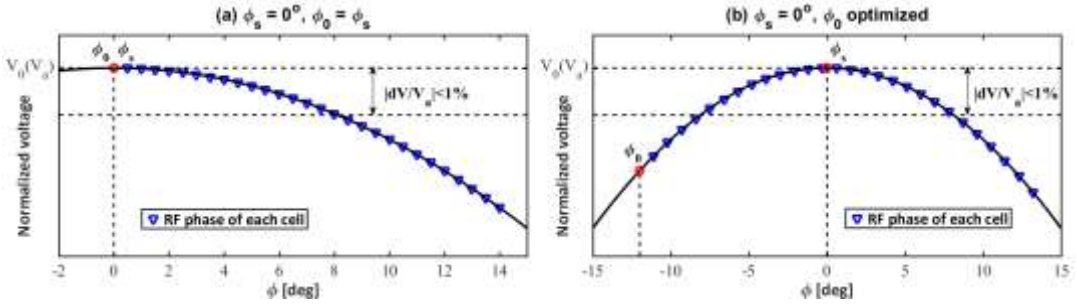

Figure 2. Distribution of the RF phase of each cell for the voltage error of 1% when (a) φ_0 is equal to φ_s and (b) φ_0 is optimized to minimize the voltage error.

II.1 Systematic temperature errors

The operating temperature of the accelerating structure is controlled by the water-cooling system. The deviation of the temperature from the nominal one has a systematic effect on the accelerating structure. For an expanded cell working at higher temperature than the nominal one, the dispersion curve will shift down, as shown in Figure 3. The impact on the RF phase caused by the temperature errors is given by Equation (3), where $\Delta\Phi_0$ is the nominal phase advance of each cell ($2\pi/3$) and α is the copper thermal expansion coefficient, which is 17 μm/m/K. The distributions of group velocity and normalized gradient of CLIC-K used to calculate the tolerances are presented in Figure 4. The same analysis has also been applied to the CLIC-G* and CLIC-380 structures.

$$\left.\begin{array}{c}\delta\varphi_c^j=L_c\delta k_c^j+k_c^j\delta L_c\\ k_c^j=\omega_0/c, L_c=\Delta\Phi_0 c/\omega_0, \delta L_c=L_c\alpha\delta T\\ \delta k_c^j=-\left(dk_z/d\omega\right)\delta\omega_c=\omega_0\alpha\delta T/v_g^j\end{array}\right\}\Rightarrow\delta\varphi_c^j=\left(1+\frac{c}{v_g^j}\right)\Delta\Phi_0\alpha\delta T \tag{3}$$

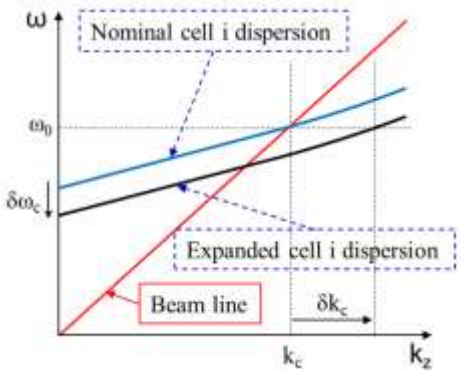

Figure 3. Dispersion curves of nominal cell and expanded cell.

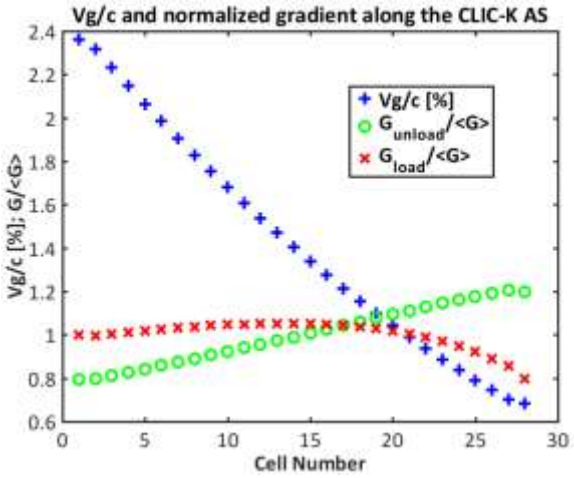

Figure 4. The distributions of group velocity and normalized unloaded and loaded gradient in CLIC-K.

Four different cases have been considered for the temperature errors. The distributions of the RF phase in each cell for these four cases are shown in Figure 5 for the unloaded gradient profile in CLIC-K structure. First, the RF input phase φ_0 is equal to the designed synchronous phase φ_s. For the on-crest case where φ_s is 0 degree, the acceptable temperature error is 3.25 K in the unloaded case to satisfy the accelerating voltage requirement: dV/V<1%. For the off-crest operation where φ_s is equal to 30 degrees, which is the maximum value foreseen for operation in the CLIC main linac, the tolerance on the temperature, 0.47 K, is much more tight due to the more critical acceptable phase error for the same voltage error limited to less than 1%. If φ_0 is optimized, the required tolerances can be less critical. For the on-crest case, the voltage error can never be fully corrected by optimizing φ_0 because every cell is working on the maximum accelerating voltage in the nominal condition. Nevertheless, the acceptable temperature error is 5.95 K which is larger than for the non-optimized φ_0. For the off-crest operation, the deviation of accelerating voltage can always be corrected by optimizing φ_0 to utilize the cell-to-cell voltage compensation if the deviation of the temperature from the nominal one is less than 22.2 K in the unloaded case. Under the requirement of less than 1% and 2% accelerating voltage errors, the tolerances on the systematic temperature errors for four different conditions in both unloaded and loaded case in CLIC-K are summarized in Table 2.

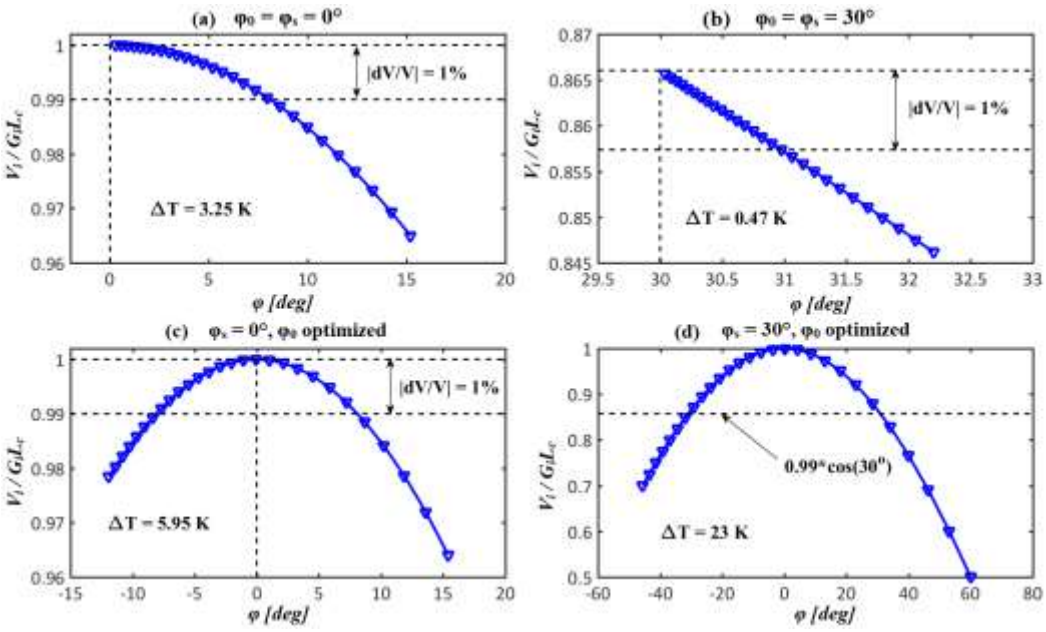

Figure 5. The distributions of the RF phase and accelerating voltage error in each cell caused by systematic temperature errors in the unloaded case for the four different conditions in CLIC-K.

Table 2. Tolerances on systematic temperature errors given by accelerating voltage error limited to < 1% and < 2% in CLIC-K.

Cases in CLIC-K			Systematic |ΔT| [K]	
			$\|\Delta V/V_0\| < 1\%$	$\|\Delta V/V_0\| < 2\%$
$\varphi_0 = \varphi_s$	$\varphi_s = 0^\circ$	Unloaded	3.25	4.60
		Loaded	3.57	5.07
	$\varphi_s = 30^\circ$	Unloaded	0.47	0.95
		Loaded	0.53	1.07
φ_0 optimized	$\varphi_s = 0^\circ$	Unloaded	5.95	8.43
		Loaded	6.21	8.81
	$\varphi_s = 30^\circ$	Unloaded	23.0	23.7
		Loaded	24.1	24.9

II.2 Systematic geometrical errors

The RF phase errors are also caused by the geometrical errors in the process of fabrication. The error distributions can be divided into two categories: systematic geometrical errors and random geometrical errors. The effect caused by systematic geometrical errors is analyzed in the following part.

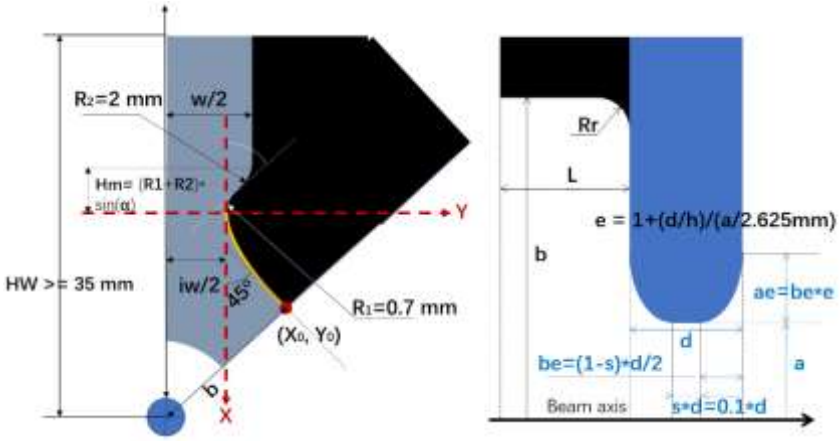

Figure 6. Sketch of a single cell geometry.

Table 3. Sensitivity of the frequency to geometrical error for different dimensions in the middle cell of CLIC-K.

Dimension x	df/dx [MHz/mm]		
	First cell	Middle cell	Last cell
b	-1157.13	-1142.59	-1127.41
a	442.34	323.40	205.53
iw	-291.37	-293.96	-298.23
w	-35.64	-34.45	-32.52
L	-64.74	-40.76	-23.14
d	161.83	101.78	54.01
Rr	114.36	105.40	97.39
R1	23.93	25.19	25.86
R2	2.55	2.62	2.62

The sketch of a single cell geometry is illustrated in Figure 6. The frequency of the cell is determined by a number of dimensions. The tolerances are dominated by the most critical geometrical parameter, which is the inner radius b of the cell, as presented in Table 3. The relationship between the phase advance of one cell and the frequency is shown in Figure 7. The RF phase errors caused by the geometrical errors can be calculated by Equation (4).

$$\left.\begin{aligned} \delta\varphi_c^j &= L_c \delta k_c^j, L_c = \frac{\Delta\Phi_0}{2\pi}\frac{c}{f_0} \\ \delta k_c^j &= -\frac{dk_z}{d\omega}\frac{d\omega}{df}\delta f = -\frac{2\pi}{v_g^j}\frac{df}{dx}\delta x \end{aligned}\right\} \Rightarrow \delta\varphi_c^j = -\frac{\Delta\Phi_0}{f_0}\frac{c}{v_g^j}\frac{df}{dx}\delta x \tag{4}$$

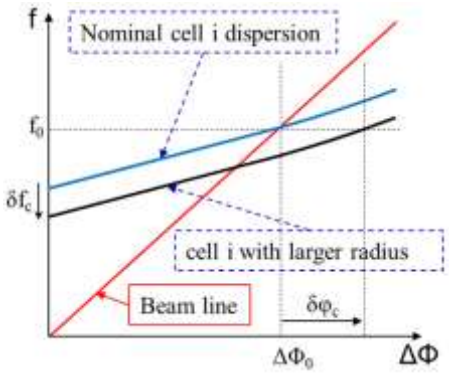

Figure 7. Dispersion curves of nominal cell and cell with larger radius.

The tolerances on the systematic geometrical errors of the most critical dimension b for four different conditions in both unloaded and loaded case to satisfy the limited accelerating voltage errors < 1% and < 2% are summarized in Table 4. The distributions of the RF phase of each cell for the same four cases as in the previous section in the unloaded case of CLIC-K are shown in Figure 8.

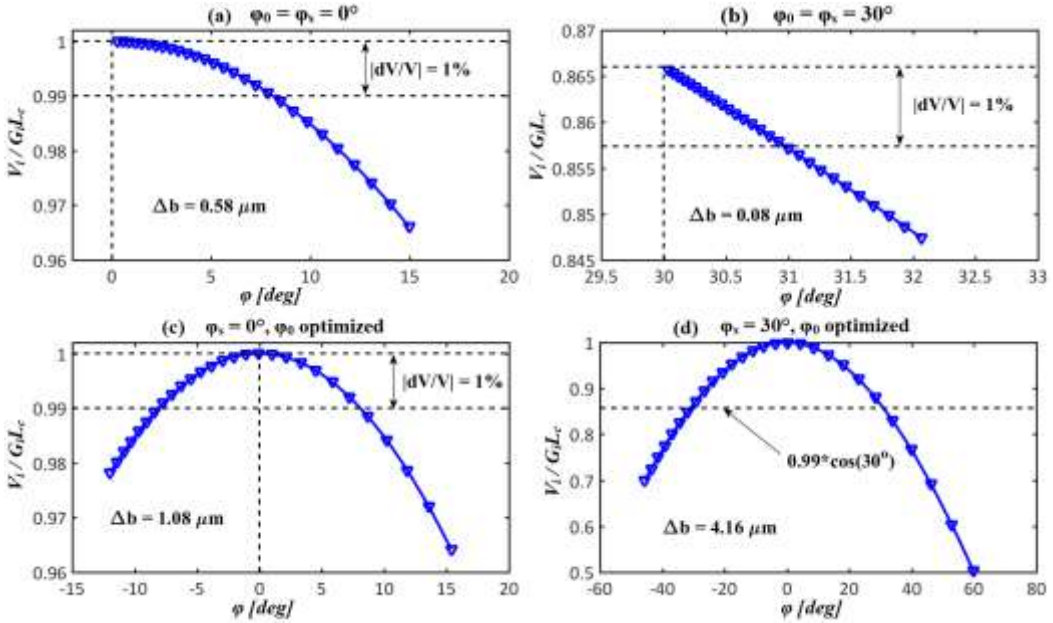

Figure 8. The distributions of the RF phase and accelerating voltage error of each cell caused by systematic geometrical errors in the beam unloaded case for the four different conditions in CLIC-K.

Table 4. Tolerances on systematic geometrical errors given by accelerating voltage error limited to < 1% and < 2% in CLIC-K.

Cases in CLIC-K			Systematic |Δb| [μm]	
			$\|\Delta V/V_0\| < 1\%$	$\|\Delta V/V_0\| < 2\%$
$\varphi_0 = \varphi_s$	$\varphi_s = 0^\circ$	Unloaded	0.58	0.83
		Loaded	0.64	0.91
	$\varphi_s = 30^\circ$	Unloaded	0.08	0.17
		Loaded	0.09	0.19
φ_0 optimized	$\varphi_s = 0^\circ$	Unloaded	1.08	1.53
		Loaded	1.13	1.60
	$\varphi_s = 30^\circ$	Unloaded	4.16	4.30
		Loaded	4.36	4.51

The systematic errors caused by the deviation of the temperature and of the geometry have similar impact on the accelerating voltage. Consequently, the temperature can be used to compensate the systematic geometrical errors on average along the structure. The compensation relationship between the temperature and systematic geometrical errors in CLIC-K is shown in Figure 9. 5.54 K temperature can compensate for 1 μm systematic errors on the most critical dimension b in CLIC-K. Even the deviation of the accelerating voltage caused by 20 μm systematic errors on dimension b can be corrected to be below 0.01% by temperature correction of -110.5 K. The distributions of the RF phase of each cell for this case is shown in Figure 10 for illustration only, since in practice such a large temperature correction is unlikely to be used.

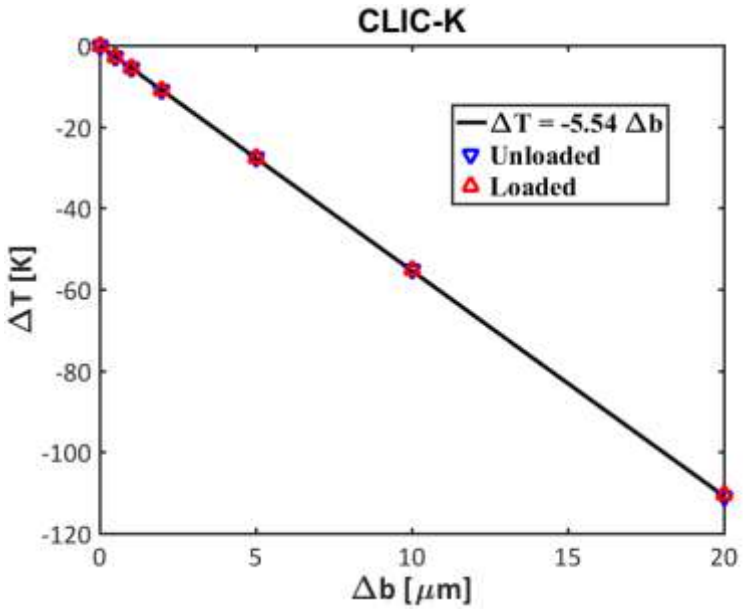

Figure 9. Accelerating voltage compensation for systematic geometrical errors on dimension b by temperature in CLIC-K.

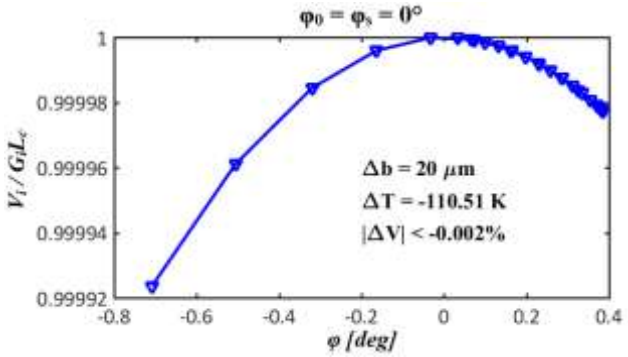

Figure 10. The distributions of the RF phase and accelerating voltage error of each cell caused by systematic geometrical errors in the beam unloaded case of CLIC-K after the compensation from temperature.

II.3 Random geometrical errors

The change in the nominal accelerating voltage caused by the random geometrical errors has also been investigated. As an example, the most critical dimension b has been taken for the following analysis but it is applicable to any dimension or to any combination of the dimensions resulting to the same frequency error.

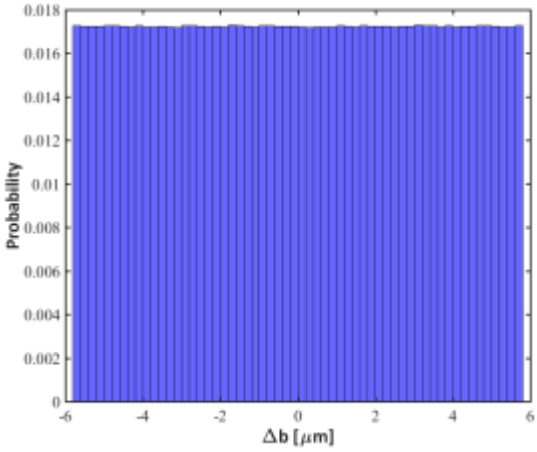

Figure 11. Uniform distribution of the random geometrical errors on dimension b.

The distribution of the random geometrical errors on dimension b is assumed to be uniform, as shown in Figure 11. For the condition where φ_0 is equal to φ_s, the distributions of accelerating voltage errors of 1 million seeds in the structure CLIC-K are presented in Figure 12(a) and 12(b). The tolerance is given when the width of half maximum of the voltage deviation is 1%. For φ_0 is optimized, the impact of the random geometrical errors on dimension b is analyzed with 30 thousand seeds. In the case of to φ_s=0, the tolerance is slightly larger compared in the case of optimized φ_0. For the off-crest case of φ_s=30 degree, it can be concluded from Figure 12(d) that the accelerating voltage error caused by random geometrical errors on the dimension b can always be corrected by adjusting the RF input phase. The distributions of optimized RF input phase φ_0 for 0 degree and 30 degrees synchronous phase in beam loaded case of CLIC-K are illustrated in Figure 13.

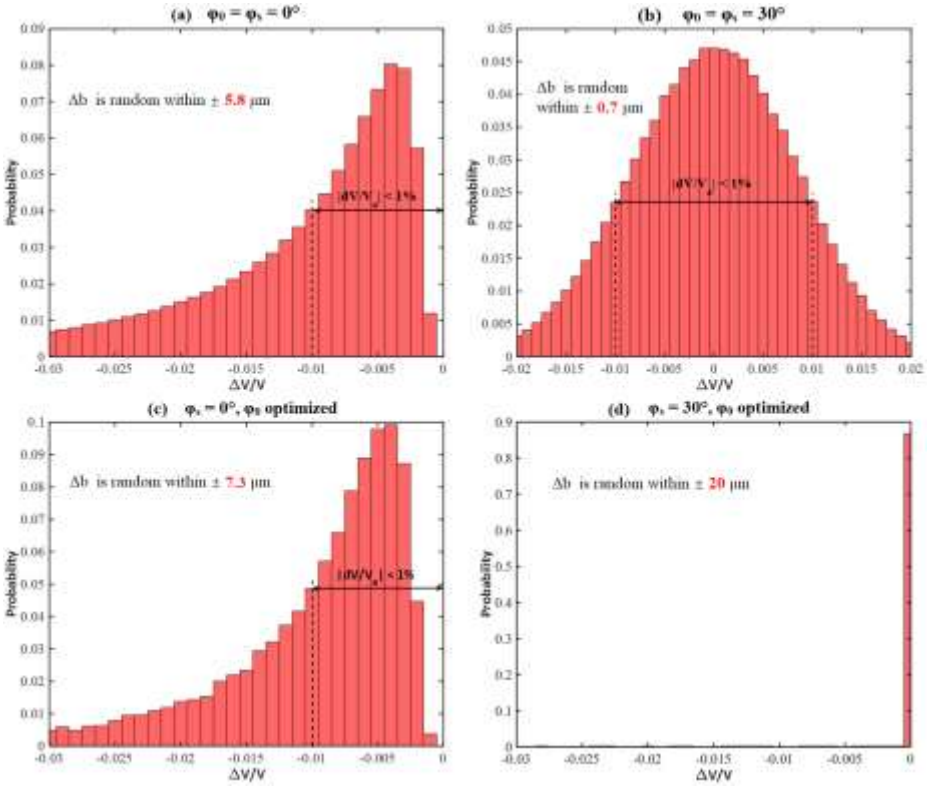

Figure 12. The distributions of accelerating voltage errors caused by random geometrical errors for the four different cases in the loaded CLIC-K.

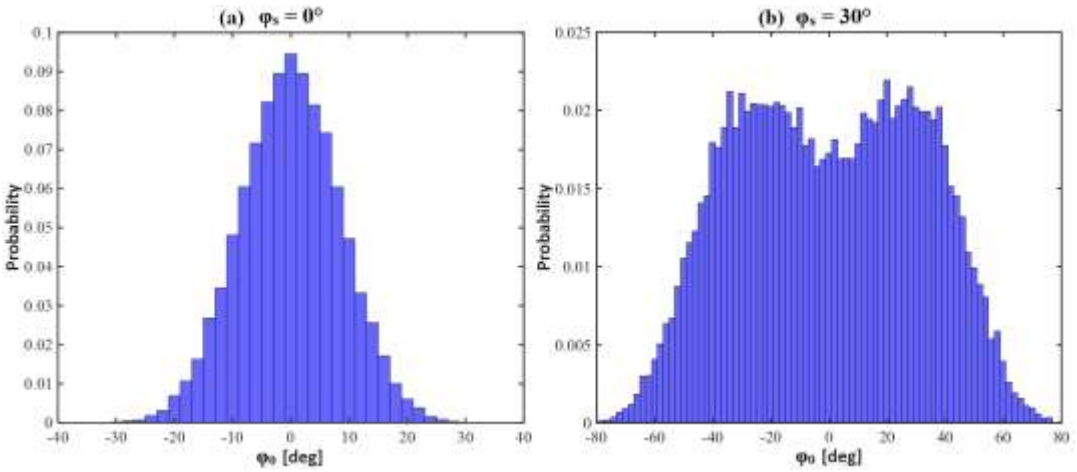

Figure 13. The distributions of optimized RF input phase φ_0 for two different synchronous phase in loaded case of CLIC-K.

Table 5. Tolerances on random geometrical errors given by limited < 1% and < 2% accelerating voltage error in CLIC-K.

Cases in CLIC-K			Random |Δb| [μm]	
			$\|\Delta V/V_0\| < 1\%$	$\|\Delta V/V_0\| < 2\%$
$\varphi_0 = \varphi_s$	$\varphi_s = 0^\circ$	Unloaded	5.5	7.8
		Loaded	5.8	8.2
	$\varphi_s = 30^\circ$	Unloaded	0.63	1.3
		Loaded	0.70	1.4
φ_0 optimized	$\varphi_s = 0^\circ$	Unloaded	7.1	10.2
		Loaded	7.3	10.5
	$\varphi_s = 30^\circ$	Unloaded	Corrected	Corrected
		Loaded	Corrected	Corrected

The tolerances on the random geometrical errors of the most critical dimension b for four different conditions and three structures in both unloaded and loaded cases in CLIC-K are summarized in Table 5.

III. Tolerances given by the acceptable reflections

The machining errors on the geometry will also lead to the reflections along the structure. The reflections will introduce standing waves in the structure, which will enhance the local field as shown in Figure 14. This may increase the breakdown rate. Consequently, the tolerances on the geometry errors is necessary to be investigate to ensure the high-gradient performance. The acceptable reflection should be below -40 dB in order to keep the local field enhancement caused by the reflections below 1%. The reflection caused by the deviation of frequency from the nominal one is analyzed in [8]. The local reflection caused by geometrical error in n-th cell is expressed in Equation (5). Seen in front of m-th cell, this local reflection is expressed in Equation (6), where α(n) is the attenuate due to the ohmic loss. The total reflection seen in front of m-th cell is calculated by adding up all the reflections caused by the geometrical errors of the downstream cells, as presented in Equation (7). When m = 1, it is written as Equation (8), which means the global reflection at the input port. Moreover, we also concern about the maximum reflection along the full structure, as expressed in Equation (9).

$$\Delta S_{11}^{local}(n) = j\frac{c}{v_g(n)}\frac{\Delta\Phi_0}{f_0}\frac{df}{dx}\delta x \tag{5}$$

$$\Delta S_{11}^{n\to m}(n)=e^{-j2(n-m)\Delta\Phi_0}e^{\alpha(n)}\Delta S_{11}^{local}(n),\alpha(n)=-\sum_{p=m}^{n-1}\frac{c\Delta\Phi_0}{v_g(p)Q_0(p)} \tag{6}$$

$$\Delta S_{11}^{global}(\mathrm{m})=\sum_{n=\mathrm{m}}^{N}\Delta S_{11}^{\mathrm{n}\to m}(n) \tag{7}$$

$$\Delta S_{11}^{global}(1)=\sum_{n=1}^{N}\Delta S_{11}^{\mathrm{n}\to 1}(n) \tag{8}$$

$$\max(\Delta S_{11})=\max\left\{\Delta S_{11}^{global}(1),\Delta S_{11}^{global}(2),\Delta S_{11}^{global}(3),...\Delta S_{11}^{global}(N)\right\} \tag{9}$$

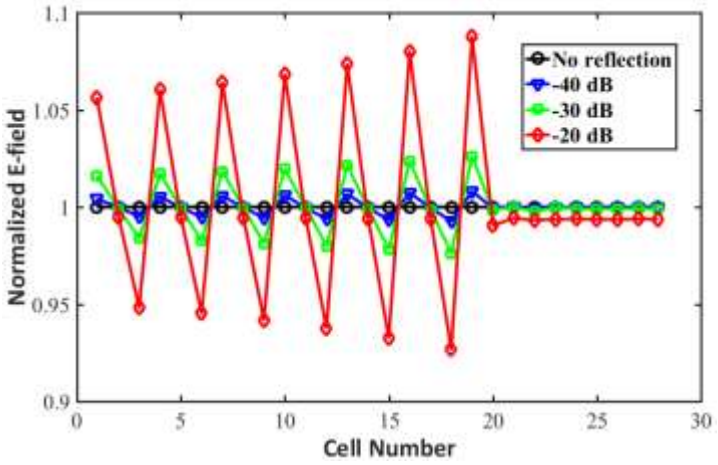

Figure 14. The impact of the reflections from the twentieth cell on the distribution of electric field along the structure with same input amplitude.

The tolerance of each cell on the most critical dimension b to keep the local reflection less than -40 dB in CLIC-K is presented in Figure 15. It is obvious that the tightest tolerance, 0.35 μm, is given by the last cell due to the lowest group velocity. For random geometrical errors, the tolerances can be given by limiting the global reflection seen at input port (Eq.8) and the maximum reflection along the structure (Eq. 9). The latter tolerance is more critical than the former one. The distributions of global reflection and maximum reflection in CLIC-K are shown in Figure 16 and 17. The tolerances on the most critical dimension b for three different level of reflections are summarized in Table 6.

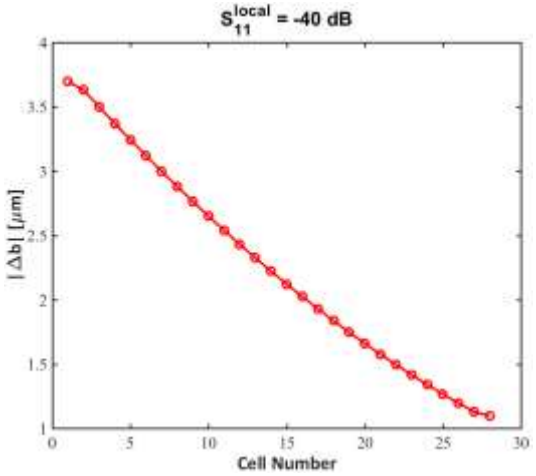

Figure 15. The tolerance of each cell on dimension b given by -40 dB local reflection in CLIC-K

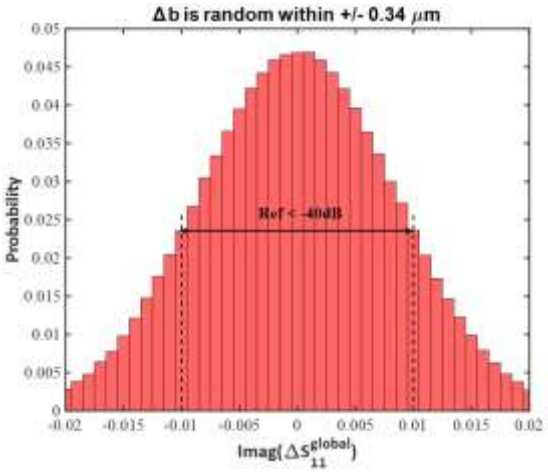

Figure 16. The distribution of global reflection at input port in CLIC-K when geometrical error on dimension b is random within ± 0.34 μm.

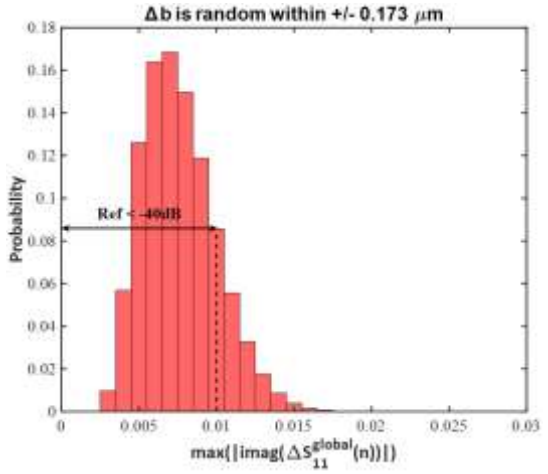

Figure 17. The distribution of maximum reflection along the structure CLIC-K when geometrical error on dimension b is random within ± 0.173 μm.

Table 6. The tolerances on the dimension b giving by limiting the reflection below -40 dB, -30 dB and -20 dB in CLIC-K.

CLIC-K	Random |Δb| [μm]		
	Γ = -40 dB	Γ = -30 dB	Γ = -20 dB
Local reflection in Eq. (5)	0.35	1.10	3.46
Global reflection at input port in Eq. (8)	0.34	1.07	3.47
Maximum reflection along structure in Eq. (9)	0.173	0.54	1.74

IV. Summary

The tolerance study for the single accelerating structure has been carried out. Two effects on the performance of the accelerating structure have been investigated: the change in the nominal accelerating voltage and the change in the field distribution along the structure. The tolerances given by the change in the nominal accelerating voltage caused by systematic temperature errors, systematic geometrical errors and random geometrical errors have been analyzed. The temperature can be used to compensate the systematic geometrical errors on the average along the structure due to the similar impact on the

accelerating voltage. The deviation of the accelerating voltage caused by the random geometrical errors can be corrected by optimizing the RF input phase. The reflections in the structure which will enhance the local field and increase the breakdown rate can be divided into three categories: local reflection, global reflection at input port and the maximum reflection along the structure. Limiting the reflection below -40 dB requires that the tolerance on the most critical dimension b should be less than 0.5 μm. In the future, more complicated tolerance study on the AS-to-AS errors will be conducted.

Appendix I

The same analysis has also been done for the CLIC-G* structure. The tolerances for systematic temperature errors, systematic and random geometrical errors, and acceptable reflections are following.

Table 7. Tolerances on systematic temperature errors given by accelerating voltage error limited to < 1% and < 2% in CLIC-G*.

Cases in CLIC-G*			Systematic $\|\Delta T\|$ [K]	
			$\|\Delta V/V_0\| < 1\%$	$\|\Delta V/V_0\| < 2\%$
$\varphi_0 = \varphi_s$	$\varphi_s = 0^\circ$	Unloaded	3.06	4.33
		Loaded	3.29	4.66
	$\varphi_s = 30^\circ$	Unloaded	0.43	0.85
		Loaded	0.47	0.93
φ_0 optimized	$\varphi_s = 0^\circ$	Unloaded	5.75	8.15
		Loaded	5.92	8.39
	$\varphi_s = 30^\circ$	Unloaded	22.2	22.9
		Loaded	22.9	23.6

Table 8. Sensitivity between the frequency and different dimensions in the middle cell of CLIC-G*.

Dimension x	df/dx [MHz/mm]		
	First cell	Middle cell	Last cell
b	-1132.72	-1097.91	-1027.65
a	355.29	284.84	209.79
iw	-299.21	-323.61	-360.05
w	-42.96	-46.95	-73.96
L	-48.13	-35.79	-24.82
d	109.99	77.60	47.29
Rr	106.85	103.92	99.64
R1	26.09	26.68	26.16
R2	2.72	3.40	3.50

Table 9. Tolerances on systematic geometrical errors given by accelerating voltage error limited to < 1% and < 2% in CLIC-G*.

Cases in CLIC-G*			Systematic $\|\Delta b\|$ [μm]	
			$\|\Delta V/V_0\| < 1\%$	$\|\Delta V/V_0\| < 2\%$
$\varphi_0 = \varphi_s$	$\varphi_s = 0^\circ$	Unloaded	0.57	0.81
		Loaded	0.62	0.87
	$\varphi_s = 30^\circ$	Unloaded	0.08	0.16
		Loaded	0.09	0.17
φ_0 optimized	$\varphi_s = 0^\circ$	Unloaded	1.09	1.55
		Loaded	1.12	1.59

$\varphi_s = 30^\circ$	Unloaded	4.22	4.35
	Loaded	4.34	4.48

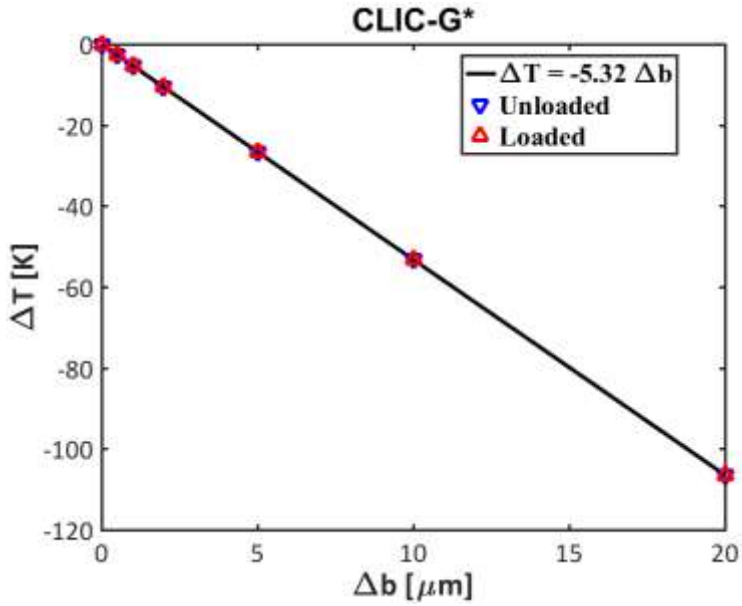

Figure 18. Accelerating voltage compensation for systematic geometrical errors on dimension b by temperature in CLIC-G*.

Table 10. Tolerances on random geometrical errors given by limited < 1% and < 2% accelerating voltage error in CLIC-G*.

Cases in CLIC-G*			Random |Δb| [μm]	
			$\|\Delta V/V_0\| < 1\%$	$\|\Delta V/V_0\| < 2\%$
$\varphi_0 = \varphi_s$	$\varphi_s = 0^\circ$	Unloaded	5.5	7.9
		Loaded	5.7	8.2
	$\varphi_s = 30^\circ$	Unloaded	0.58	1.18
		Loaded	0.62	1.27
φ_0 optimized	$\varphi_s = 0^\circ$	Unloaded	7.3	10.4
		Loaded	7.5	10.5
	$\varphi_s = 30^\circ$	Unloaded	Corrected	Corrected
		Loaded	Corrected	Corrected

Table 11. The tolerances on the dimension b giving by limiting the reflection below -40 dB, -30 dB and -20 dB in CLIC-G*.

CLIC-K	Random |Δb| [μm]		
	Γ = -40 dB	Γ = -30 dB	Γ = -20 dB
Local reflection in Eq. (5)	0.47	1.48	4.68
Global reflection at input port in Eq. (8)	0.34	1.11	3.49
Maximum reflection along structure in Eq. (9)	0.186	0.59	1.89

Appendix II

In this part, the results of tolerances in CLIC-380 is summarized.

Table 12. Tolerances on systematic temperature errors given by accelerating voltage error limited to < 1%

and < 2% in CLIC-380.

Cases in CLIC-380			Systematic |ΔT| [K]	
			$\|\Delta V/V_0\| < 1\%$	$\|\Delta V/V_0\| < 2\%$
$\varphi_0 = \varphi_s$	$\varphi_s = 0^\circ$	Unloaded	3.63	5.14
		Loaded	4.01	5.68
	$\varphi_s = 30^\circ$	Unloaded	0.51	1.01
		Loaded	0.58	1.14
φ_0 optimized	$\varphi_s = 0^\circ$	Unloaded	6.76	9.58
		Loaded	7.06	10.0
	$\varphi_s = 30^\circ$	Unloaded	26.1	26.9
		Loaded	27.3	28.2

Table 13. Sensitivity between the frequency and different dimensions in the middle cell of CLIC-380.

Dimension x	df/dx [MHz/mm]		
	First cell	Middle cell	Last cell
b	-993.47	-1021.85	-1043.77
a	491.20	328.38	270.14
iw	-383.50	-371.68	-336.54
w	-108.13	-75.41	-60.64
L	-78.07	-48.71	-40.51
d	214.78	145.47	86.98
Rr	133.89	103.57	108.36
R1	27.42	34.12	36.15
R2	4.02	3.78	3.51

Table 14. Tolerances on systematic geometrical errors given by accelerating voltage error limited to < 1% and < 2% in CLIC-380.

Cases in CLIC-380			Systematic |Δb| [μm]	
			$\|\Delta V/V_0\| < 1\%$	$\|\Delta V/V_0\| < 2\%$
$\varphi_0 = \varphi_s$	$\varphi_s = 0^\circ$	Unloaded	0.74	1.04
		Loaded	0.82	1.15
	$\varphi_s = 30^\circ$	Unloaded	0.10	0.20
		Loaded	0.12	0.23
φ_0 optimized	$\varphi_s = 0^\circ$	Unloaded	1.36	1.93
		Loaded	1.42	2.01
	$\varphi_s = 30^\circ$	Unloaded	5.25	5.42
		Loaded	5.51	5.68

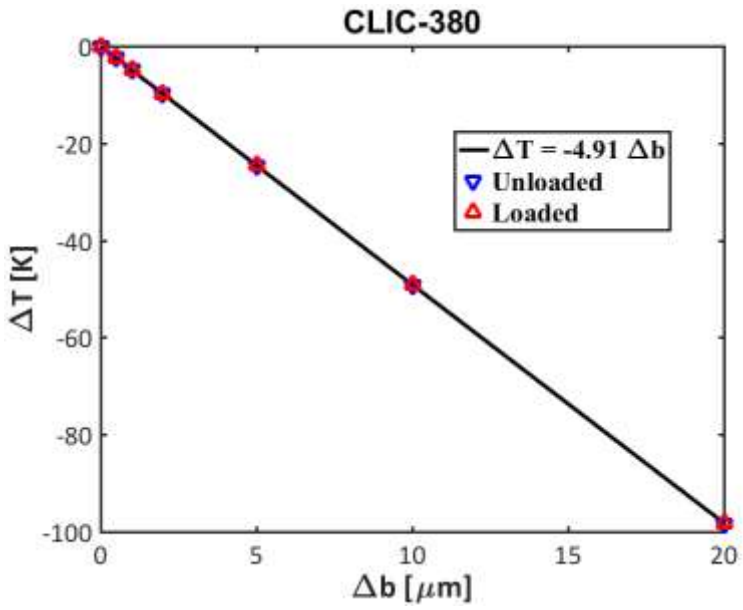

Figure 19. Accelerating voltage compensation for systematic geometrical errors on dimension b by temperature in CLIC-380.

Table 15. Tolerances on random geometrical errors given by limited < 1% and < 2% accelerating voltage error in CLIC-380.

Cases in CLIC-380			Random |Δb| [μm]	
			$\|\Delta V/V_0\| < 1\%$	$\|\Delta V/V_0\| < 2\%$
$\varphi_0 = \varphi_s$	$\varphi_s = 0^\circ$	Unloaded	7.6	10.8
		Loaded	7.9	11.3
	$\varphi_s = 30^\circ$	Unloaded	0.87	1.75
		Loaded	0.96	1.93
φ_0 optimized	$\varphi_s = 0^\circ$	Unloaded	9.6	13.6
		Loaded	10.1	14.6
	$\varphi_s = 30^\circ$	Unloaded	Corrected	Corrected
		Loaded	Corrected	Corrected

Table 16. The tolerances on the dimension b giving by limiting the reflection below -40 dB, -30 dB and -20 dB in CLIC-380.

CLIC-380	Random |Δb| [μm]		
	Γ = -40 dB	Γ = -30 dB	Γ = -20 dB
Local reflection in Eq. (5)	0.52	1.65	5.21
Global reflection at input port in Eq. (8)	0.34	1.07	3.47
Maximum reflection along structure in Eq. (9)	0.234	0.74	2.34

References

[1] CLIC Collaboration, CLIC Conceptual Design Report: A Multi-TeV Linear Collider Based on CLIC Technology, Report No. CERN-2012-007, 2012.

[2] CLIC and CLICdp Collaborations, Updated Baseline for a Staged Compact Linear Collider, Report No. CERN-2016-004, 2016

[3] A. Grudiev, W. Wuensch, Design of the CLIC Main Linac Accelerating Structure for CLIC Conceptual Design Report, *Proceeding of LINAC10*, Tsukuba, Japan, pp. 211-213, 2010.

[4] H. Zha, A. Grudiev, Design and optimization of Compact Linear Collider main linac accelerating structure, Physical Review Accelerators And Beams. 19 (2016). doi:10.1103/physrevaccelbeams.19.111003.

[5] X. Huang, A. Grudiev, Z. Zhao et al., CLIC380: RF design and parameters of 2017 re-baselined 380 GeV CLIC linac accelerating structure, Nuclear Inst. And Methods in Physics Research, A (2018), https://doi.org/10.1016/j.nima.2018.11.104.

[6] J. Liu, A. Grudiev, RF design of accelerating structure for the main linac of the klystron-based first stage of CLIC at 380 GeV, CLIC-Note-1082, 2018.

[7] D. Schulte, private communication.

[8] J. Shi, A. Grudiev and W. Wuensch, Tuning of X-band traveling-wave accelerating structures, *Nuclear Instruments and Methods in Physics Research Section A: Accelerators, Spectrometers, Detectors and Associated Equipment*, vol. 704, pp. 14-18, 2013.